British Journal of Pharmacology

DOI:10.1111/bph.13393
www.brjpharmacol.org

RESEARCH PAPER

Involvement of transglutaminase 2 and voltage-gated potassium channels in cystamine vasodilatation in rat mesenteric small arteries

Morten Engholm, Estéfano Pinilla, Susie Mogensen, Vladimir Matchkov, Elise Røge Hedegaard, Hua Chen, Michael J Mulvany and Ulf Simonsen

Department of Biomedicine, Pulmonary and Cardiovascular Pharmacology, Aarhus University, Denmark

Correspondence
Ulf Simonsen, Department of Biomedicine, Aarhus University, Wilhelm Meyers Allé 4, 8000 Aarhus C, Denmark.
E-mail: us@biomed.au.dk

Received
7 February 2015
Revised
13 October 2015
Accepted
10 November 2015

BACKGROUND AND PURPOSE

Vasodilatation may contribute to the neuroprotective and vascular anti-remodelling effect of the tissue transglutaminase 2 (TG2) inhibitor cystamine. Here, we hypothesized that inhibition of TG2 followed by blockade of smooth muscle calcium entry and/or inhibition of Rho kinase underlies cystamine vasodilatation.

EXPERIMENTAL APPROACH

We used rat mesenteric small arteries and RT-PCR, immunoblotting, and measurements of isometric wall tension, intracellular Ca^{2+} ($[Ca^{2+}]_i$), K^+ currents (patch clamp), and phosphorylation of myosin phosphatase targeting subunit 1 (MYPT1) and myosin regulatory light chain, in our experiments.

KEY RESULTS

RT-PCR and immunoblotting revealed expression of TG2 in mesenteric small arteries. Cystamine concentration-dependently inhibited responses to phenylephrine, 5-HT and U46619 and for extracellular potassium. Selective inhibitors of TG2, LDN 27129 and T101, also inhibited phenylephrine contraction. An inhibitor of PLC suppressed cystamine relaxation. Cystamine relaxed and reduced $[Ca^{2+}]_i$ in phenylephrine-contracted arteries. In potassium-contracted arteries, cystamine induced less relaxation without changing $[Ca^{2+}]_i$, and these relaxations were blocked by mitochondrial complex inhibitors. Blockers of K_v7 channels, XE991 and linopirdine, inhibited cystamine relaxation and increases in voltage-dependent smooth muscle currents. Cystamine and the Rho kinase inhibitor Y27632 reduced basal MYPT1-Thr^{855} phosphorylation, but only Y27632 reduced phenylephrine-induced increases in MYPT1-Thr^{855} and myosin regulatory light chain phosphorylation.

CONCLUSIONS AND IMPLICATIONS

Cystamine induced vasodilatation by inhibition of receptor-coupled TG2, leading to opening of K_v channels and reduction of intracellular calcium, and by activation of a pathway sensitive to inhibitors of the mitochondrial complexes I and III. Both pathways may contribute to the antihypertensive and neuroprotective effect of cystamine.

Abbreviations

TG2, transglutaminase 2; MLC, myosin light chain; MLCK, myosin light chain kinase; MLCP, myosin light chain phosphatase; MYPT1, myosin phosphatase target subunit 1; p-MYPT1, phosphorylated form of MYPT1; MLC2, myosin regulatory light chain; p-MLC2, phosphorylated form of MLC2; ROCK, Rho-associated protein kinase

Tables of Links

TARGETS
Voltage-gated Ion Channels[a]
K_v7 channels
Enzymes[b]
MLCK, myosin light chain kinase
ROCK, Rho kinase

LIGANDS
4-Aminopyridine (fampridine)
Glibenclamide
Linopirdine
TEA, tetraethylammonium
XE991
Y27632

These Tables list key protein targets and ligands in this article which are hyperlinked to corresponding entries in http://www.guidetopharmacology.org, the common portal for data from the IUPHAR/BPS Guide to PHARMACOLOGY (Pawson *et al.*, 2014) and are permanently archived in the Concise Guide to PHARMACOLOGY 2015/16 ([a,b]Alexander *et al.*, 2015a,b).

Introduction

In recent years, interest in the small organic disulphide cystamine has increased, because this compound and its reduced derivative cysteamine, have been shown to be neuroprotective, to increase survival, to improve motor performance in Huntington's disease (Dedeoglu *et al.*, 2002; Karpuj *et al.*, 2002) and to reduce neuronal loss in animal models of Parkinson's disease (Stack *et al.*, 2008; Gibrat *et al.*, 2010). The therapeutic benefits mediated by cystamine have, in part, been attributed to inhibition of transglutaminase 2 (TG2) (Jeitner *et al.*, 2005). TG2 mediates covalent cross-links of structural proteins (Lorand and Graham, 2003), acts as a G-protein (G_h) in transmembrane signalling (Fesus and Piacentini, 2002) and is involved in cell proliferation, cell adhesion, apoptosis, cell–matrix interactions and reorganization of extracellular matrix (Griffin *et al.*, 2002). Small artery remodeling also depends on TG2 (Bakker *et al.*, 2005), and administration of cystamine, which inhibits TG2 competitively by binding to the active site and acting as an alternative substrate (Jeitner *et al.*, 2005), has been shown to inhibit eutrophic inward remodelling in phenylephrine-induced hypertensive rats (Eftekhari *et al.*, 2007) and to reduce BP in spontaneously hypertensive rats (Engholm *et al.*, 2011). However, it is not known whether inhibition of remodelling by cystamine is mediated only through its effect on extracellular TG2 or inhibition of vasoconstriction (Eftekhari *et al.*, 2007). There are seven different transglutaminases (TG1–TG7 encoded by *tgm1–tgm7*), and recently, TG1 and TG4 were found to be expressed in rat aorta and vena cava smooth muscle (Johnson *et al.*, 2012), but it is unclear whether these transglutaminases contribute to the vascular effect of cystamine in resistance arteries.

Vascular tone is dependent on the relative activities of myosin light chain (MLC) kinase (MLCK) and myosin light chain phosphatase (MLCP), where activation of MLCK or inhibition of MLCP can increase phosphorylation of MLC and thereby initiate vascular smooth muscle contraction (Somlyo and Somlyo, 2003). Phosphorylation of MLC is regulated by cytosolic Ca^{2+}, and the Ca^{2+}–calmodulin initiated activation of MLCK. Other mechanisms are also involved such as Rho-associated protein kinase (ROCK)-initiated phosphorylation of the regulatory MLCP subunit, myosin phosphatase targeting subunit 1 (MYPT1) or PKC-initiated phosphorylation of CPI-17. Both the latter mechanisms result in inhibition of MLCP activity and increased phosphorylation of MLC and hence increased vascular tone (Somlyo and Somlyo, 2003; Eto, 2009). The vasoactive effects of cystamine may possibly be mediated by altered phosphorylation of these contractile proteins.

The present study hypothesized that cystamine evokes small vessel relaxation through inhibition of TG2 followed by blockade of smooth muscle calcium entry and/or inhibition of Rho kinase. To investigate the hypothesis, the vasodilatory effects of cystamine and mechanisms involved were examined in rat small arteries as follows: (i) RT-PCR and immunoblotting were performed for expression of transglutaminases in small arteries; (ii) the vasodilatatory effect of cystamine was compared with selective cell-impermeable and cell-permeable inhibitors of TG2; (iii) simultaneous measurements of smooth muscle calcium and tension were performed; (iv) whole-cell patch clamp was conducted; (v) tension and corresponding phosphorylation of MYPT1 (Wilson *et al.*, 2005) and myosin regulatory light chain (MLC2) (Solaro, 2000) were measured; and (vi) finally, TG2 has also been suggested to act as a protein disulphide isomerase regulating mitochondrial respiratory chain function (Mastroberardino *et al.*, 2006), and therefore, the effect of mitochondrial complex inhibitors on cystamine relaxation was also tested.

Methods and materials

Animals and preparation of mesenteric arteries

All animal care and experimental protocols were approved by the National Danish Animal Experiments Inspectorate (permission 2006/561-1160 and permission 2011/561-2011) and followed the ARRIVE guidelines (McGrath and Lilley, 2015), Animals were housed in the animal facility in cages (Universal Euro III type Long) with standard wood bedding and space for two rats. There was a 12 h cycle of light and dark, and the animals had free access to food and drinking water.

The animals were selected randomly and, wherever possible, observations were made without knowledge of the treatments

administered. Adult male Wistar rats (12–14 weeks) weighing 250–300 g (Taconic Aps, Ry, Denmark) were killed by cervical dislocation by trained animal staff at Aarhus University, and the mesenteric bed was excised and immediately immersed in 4°C cold physiological saline solution (PSS, pH = 7.4) of the following composition (mM): 119 NaCl, 4.7 KCl, 1.18 KH_2PO_4, 1.17 $MgSO_4$, 1.5 $CaCl_2$, 24.9 $NaHCO_3$, 0.026 EDTA and 5.5 glucose. Mesenteric second-order branches (diameter approximately 250 μm) were dissected.

RT-PCR for transglutaminases

Rat tissue and dissected small arteries from five rats were kept in RNAlater (Qiagen, Copenhagen, Denmark) and processed as previously described (Hedegaard *et al.*, 2014). cDNA was amplified in a thermal cycler (Peqlab, Eurofins MWG Operon, Ebersberg, Germany). Controls (RT-) were performed using RNA directly in PCR without exposing the RNA to cDNA synthesis with reverse transcriptase. PCR reaction products were resolved by agarose gel electrophoresis (2.5% w v^{-1}) and stained with ethidium bromide (0.5 $\mu g \cdot mL^{-1}$). The primers and expected product size are listed in the Supporting Information Table 1. To determine the identity of the amplification products, the purified PCR product was sequenced by Eurofins MWG Operon (Hedegaard *et al.*, 2015).

Immunoblotting for TG1 and TG2

For detection of TG1 and TG2, mesenteric arteries from five rats were isolated and frozen at −80°C. The tissue was homogenized in lysis buffer (20 mM Tris/HCl, 5 mM EGTA, 150 mM NaCl, 20 mM glycerophosphate, 10 mM NaF, 1% Triton X-100, 0.1% Tween-20, 1× Halt™ protease and phosphatase inhibitor cocktail) by using a pestle; then the sample was centrifuged for 10 min at 11200 x *g* at 4°C and the supernatant frozen at −80°C. Total protein was quantified using the Bio-Rad Protein Assay (Bio-Rad, Hercules, CA, USA). Protein lysate (7 μg) was mixed with sample buffer and loaded with a prestain marker (Bio-Rad) onto the gel. For TG1, we used human TGase1 transfected 293T lysate (Sc 113816, Santa-Cruz Biotechnology, Santa Cruz, CA, USA) as a control and for TG2 human TG2 full-length protein (ab152748, Abcam, Cambridge, UK). Immunoblotting was performed as described previously (Hedegaard *et al.*, 2014). The following antibodies were applied: TG1 antibody (sc-166467, Santa-Cruz Biotechnology) 1:200, TG2 antibody (ab421, Abcam) 1:200, pan-actin antibody (#4968, Cell signalling Technology, Beverly, MA, USA) 1:1000, anti-rabbit IgG conjugated to horse radish peroxidase (HRP) (Santa-Cruz Biotechnology) 1:4000 and anti-mouse IgG conjugated to HRP (#7076, Cell signalling Technology).

Isometric tension studies

Mesenteric arteries were mounted on 40 μm stainless steel wires in a myograph system (model 410A, Danish Myo Technology, Aarhus, Denmark) containing PSS at 37°C and continuously gassed with 95% O_2–5% CO_2 (pH 7.4). The arteries were stretched to 0.9 times the estimated internal diameter at 100 mmHg for which the active tension is maximal (Mulvany and Halpern, 1977). Vessel viability was examined by stimulation with noradrenaline (5 μM) for 2 min (effective pressure >13.3 kPa) and the presence of endothelium assessed by addition of ACh (10 μM) (relaxation >75%).

Concentration–response curves were constructed for phenylephrine, 5-HT, U46619 and KPSS, where KPSS is PSS with the NaCl equivalently replaced with KCl to give the $[K^+]$ indicated. KPSS was added in combination with 1 μM phentolamine to inhibit the effects of neuronally released noradrenaline. Cystamine was then added to the bath in increasing concentrations (10^{-5}–10^{-2} M) and after 20 min, the concentration–response curves were repeated. Contraction was expressed as active wall tension, which is the increase in measured force divided by twice the segment length.

Studies of cystamine relaxation

To investigate whether TG2 is involved in the relaxations induced by cystamine, these were compared with the relaxant effect of two selective inhibitors of TG2, T101 (1,3,4,5-tetramethyl-2-[(2-oxopropyl)thio]imidazolium chloride), a non-cell-permeable substance and a cell permeable inhibitor, LDN 27219 (2-[(3,4-dihydro-4-oxo-3,5-diphenylthieno[2,3-*d*]pyrimidin-2-yl)thio]acetic acid hydrazide), before incubation with monodansylcadaverine. Preparations were incubated with monodansylcadaverine (100 μM) for 30 min and, after washout, concentration–response curves were constructed for cystamine, LDN 27219 and the PLC inhibitor, U73122.

To investigate the role of PLC, the preparations were incubated with the inhibitor U73122 (5 μM) or an inactive analogue, U73343 (10 μM), and concentration–response curves were constructed for cystamine.

To investigate whether K^+channels are involved in cystamine relaxation, the preparations were contracted with phenylephrine, and concentration–response curves for cystamine were constructed in the presence of vehicle, a blocker of calcium-activated K^+ channels, tetraethylammonium (TEA) (1 mM (Kun *et al.*, 2009)), a blocker of ATP-sensitive K channels, glibenclamide (1 μM); a blocker of voltage-gated K^+ channels, 4-aminopyridine (0.5 mM); and blockers of K_V7 channels, XE991 (10 μM) or linopirdine (10 μM). The responses were tested in parallel by mounting four vessel segments and only performing one concentration–response curve for each vasodilator.

To investigate the cystamine relaxations persisting in arteries contracted with 100 mM KPSS, the preparations were pretreated with phentolamine (1 μM) and incubated with inhibitors of mitochondrial complexes I and III, respectively, rotenone (1 μM) and antimycin A (1 μM). These inhibitors cause inhibition of contraction by themselves, and therefore, the contraction levels were adjusted by adding U46619. Inhibition of the mitochondrial chain may increase superoxide formation, and therefore, the effect of both a general superoxide scavenger, tempol, and a mitochondria-specific superoxide scavenger (mito-tempo) on cystamine relaxation was also examined.

Relaxations were expressed relative to the pre-constriction induced by, for example, phenylephrine or 100 mM KPSS.

Simultaneous measurements of $[Ca^{2+}]_i$ and tension

Simultaneous measurements of cytoplasmic calcium activity ($[Ca^{2+}]_i$) and tension were performed as described elsewhere (Buus *et al.*, 1998; Villalba *et al.*, 2007). Briefly, arterial segments (1–2 mm in length) from five rats were mounted in an isometric myograph and were incubated in the dark at 37°C in PSS containing 5 μM Fura-2AM (Molecular Probes,

Eugene, OR, USA) and the nonionic surfactants: 0.02% Pluronic F-127, 0.5% DMSO and 0.1% Cremophor EL for a 2 h period. After loading, the myograph was placed on the stage of an inverted Zeiss microscope equipped for dual excitation wavelength microfluorimetry (Deltascan; Photon Technology International, Birmingham, NJ, USA). Vessels were illuminated with alternating 340 and 380 nm light, and light emission at 510 nm was collected using a photomultiplier. Vessel viability and Ca^{2+} signal were tested for each preparation by stimulation with 100 mM KPSS.

To study the effects of cystamine on isometric tension and $[Ca^{2+}]_i$, segments were contracted with either 10 μM phenylephrine or 100 mM KPSS in combination with 1 μM phentolamine until a stable contraction was obtained. Increasing concentrations of cystamine (1–100 μM) were added with 10 min intervals. Quenching of Fura-2AM with 15 mM Mn^{2+} was performed at the end of each experiment to determine background fluorescence. $[Ca^{2+}]_i$ has been expressed as the ratio F_{340}/F_{380} corrected for background fluorescence by subtracting these values from the emission levels obtained during the experiment.

Voltage clamp

Patch clamp experiments were performed in accordance to a previous protocol (Zhong *et al.*, 2010). Rat mesenteric arteries were dissected, opened longitudinally and stored in an ice-cold dissection solution containing the following (mM): 60 NaCl, 80 sodium glutamate, 5 KCl, 2 $MgCl_2$, 10 glucose and 10 HEPES (pH 7.4). The arteries were equilibrated in dissection solution with BSA (1 $mg{\cdot}mL^{-1}$) at 37°C for 10 min and then exposed to the same solution supplemented with papain (0.5 $mg{\cdot}mL^{-1}$; Worthington Biochemical Corp., Lakewood, NJ, USA) and dithiothreitol (DTT; 1.5 $mg{\cdot}mL^{-1}$) at 37°C for 10 min and washed afterwards in an ice-cold dissociation solution. Arteries were moved to dissociation solution containing 100 μM Ca^{2+}, BSA (1 $mg{\cdot}mL^{-1}$) and collagenase (0.7 $mg{\cdot}mL^{-1}$ type F and 0.4 $mg{\cdot}mL^{-1}$ type H; Worthington Biochemical Corp.) at 37°C for 10 min. Isolated smooth muscle cells were liberated by gentle trituration of digested arteries with a fire-polished pipette into the bath solution. Isolated smooth muscle cells were used for patch clamp studies 15 min after isolation and within the next 4 h. The bath solution contained (mM) the following: 120 NaCl, 3 $NaHCO_3$, 4.2 KCl, 1.2 KH_2PO_4, 2 $MgCl_2$, 0.1 $CaCl_2$, 10 glucose and 10 HEPES (pH 7.4). The patch pipette solution contained (mM) the following: 110 potassium gluconate, 30 KCl, 0.5 $MgCl_2$, 5 HEPES, 10 EGTA, 5 Na_2ATP and 1 GTP (pH 7.2). Current–voltage (I–V) relations were determined using 500 ms step pulses to between −95 and +45 mV in increments of 10 mV at a holding potential of −65 mV. Current amplitudes in treated and control groups were normalized to peak current at +45 mV under control conditions to reduce variability resulting from cell-to-cell differences in current amplitude.

p-MYPT1/MYPT1 and p-MLC/MLC determination in mesenteric small arteries

The effect of cystamine on ROCK activity was quantified by Western blot analysis for total MYPT1 and phosphorylated MYPT1 (p-MYPT1). Mesenteric arterial segments were mounted and incubated with cystamine (100 μM), Y27632 (1 μM) (a selective inhibitor of ROCKs) or PSS alone or in combination for 20 min followed by 2 min stimulation with phenylephrine (10 μM). Vessels were then immediately immersed in ice-cold 10 mM DTT in acetone plus 10% trichloroacetic acid and stored for 24 h at −70°C. Two arterial segments from each animal were immersed in sample buffer (6 mM DTT, 350 mM Tris–HCL, 10% SDS, 30% glycerol, 0.123% bromophenol blue) mixed with (1:1) lysis buffer [20 mM Tris–HCL, 5 mM EGTA, 150 mM NaCl, 20 mM glycerophosphate, 10 mM NaF, 1% Triton X-100, 0.1% Tween-20, protease inhibitor cocktail (Thermo Scientific, Waltham, MA, USA) (pH 7.5)] and heated for 10 min at 50°C, and then they were homogenized and centrifuged at 16600 x *g* for 10 min, and the supernatant was collected. Immunoblotting was performed as described previously (Hedegaard *et al.*, 2014). The primary antibodies were for p-MYPT1 (SA19, 1:500; Millipore, Billerica, MA, USA; antibody against chicken Thr^{850}, corresponding to rat Thr^{855}) and for MYPT1 (SC25618, 1:6000; Santa Cruz Biotechnology). Total MLC2 and phosphorylated MLC2 (p-MLC2) were determined as for MYPT1 and p-MYPT1 but using the following antibodies: myosin light chain 2 antibody (clone 3672; Cell Signaling Technology) and phospho-myosin light chain 2 (Ser^{19}) antibody (clone 3671; Cell Signaling Technology). Each strip was incubated with HRP-conjugated anti-rabbit IgG (1:4000; Invitrogen, Carlsbad, CA, USA) for 120 min. In the presence of α_1 adrenoceptor activation, the densitometric measurements of MYPT1 correlated linearly with p-MYPT and MLC2 with p-MLC2, and the average expression of MYPT1 and MLC2 was similar across the different experimental groups (data not shown). Therefore, p-MYPTand p-MLC2 were expressed as ratios of their respective unphosphorylated proteins.

Data analysis

Data are expressed as means ± SEM, where *n* is the number of animals studied in each group. Concentration–response curves were analysed by repeated measures of ANOVA followed by a Bonferroni post test for multiple comparisons. One-way ANOVA was used for multiple testing followed by Bonferroni's multiple comparison *post hoc* analysis. A *P* value of <0.05 was considered significant.

Materials

The following drugs were used: ACh, 4-aminopyridine, antimycin A, cystamine, glibenclamide, 5-HT, linopirdine, monodansylcadaverine, phentolamine, phenylephrine, rotenone, sodium nitroprusside (SNP), tempol, mito-tempo (2-(2,2,6,6-tetramethylpiperidin-1-oxyl-4-ylamino)-2-oxoethyl) triphenylphosphonium chloride), TEA, U46619 (9α-epoxymethanoprostaglandin $F_{2\alpha}$) and XE991 (10,10-bis(4-pyridinylmethyl)-9(10*H*)-anthracenone dihydrochloride) from Sigma (St. Louis, MO, USA). U73122, U73343, LDN 27219 and Y27632 were obtained from Tocris Bioscience (Bristol, UK). T101 was from Zedira (Darmstadt, Germany). Fura-2AM and pluoronic F127 were purchased from Invitrogen (Taastrup, Denmark). Unless otherwise stated, the substances were dissolved in distilled water. Fresh solutions of cystamine were made each day. U73122, U73343, LDN27219, T101 and Y27632 were dissolved in DMSO and kept at −20°C and further dissolved in distilled water at the day of experiment. The DMSO concentration in the bath was below 0.01% and did not affect vascular contractility.

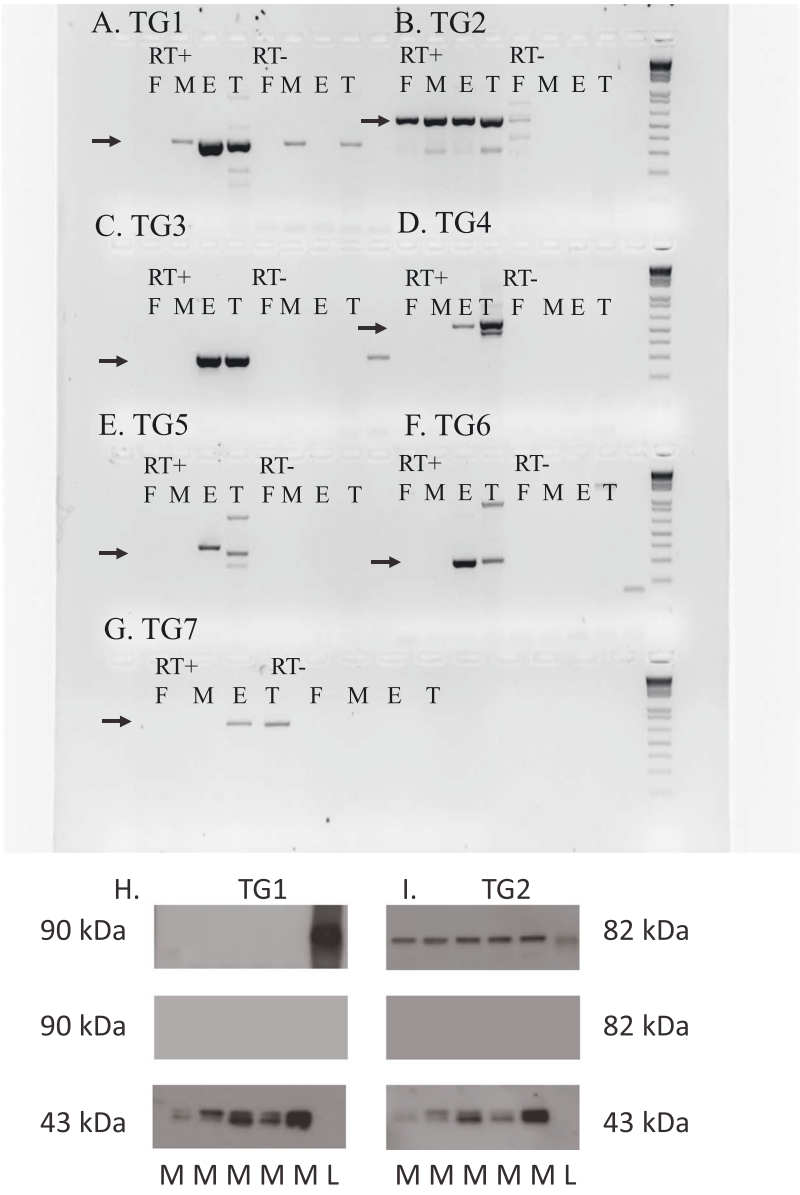

Figure 1

Detection of transglutaminases (TG1–TG7) in rat mesenteric arteries by RT-PCR and immunoblotting. (A–G) In all panels, lanes 1–4 are RT-positive samples of rat femoral small artery (F), mesenteric small artery (M), ear (E) and testes (T), and lanes 5–8 are RT-negative samples of the same tissues. The bands that were sequenced and confirmed as the right product are marked with an arrow. Primers can be seen in Supporting Information Table 1. (A) TG1, (B) TG2 (tissue transglutaminase), (C) TG3, (D) TG4, (E) TG5, (F) TG6 and (G) TG7. (H) Immunoblot of TG1 in rat mesenteric arteries located at 90 kDa (upper band). Controls with omission of primary antibody (middle band). Pan-actin located at 43 kDa (lower band). Lanes 1–5 mesenteric arteries, lane 6 human TGase1 transfected 293T lysate (L). (I) Immunoblot of TG2 in rat mesenteric arteries located at 82 kDa (upper band). Controls with omission of primary antibody (middle band). Pan-actin located at 43 kDa (lower band). In lane 6 human TG2 full length protein.

Results

RT-PCR and immunoblotting for transglutaminases

We examined the presence of TG1–TG7 mRNA by RT-PCR and sequence analysis (Figure 1A–G). In rat femoral small arteries, we only found expression of TG2, while in mesenteric small arteries, there was expression of TG2 and a weak band for TG1. Skin from the rat ear and testes were included as positive control tissues and showed expression of TG1–TG7, although in ear skin, the band size and sequence did not correspond to TG5 (Figure 1E).

Immunoblotting for TG1 and TG2 protein revealed only the expression of TG2 in rat mesenteric arteries, while TG1 was only expressed in the positive control samples (Figure 1H, I).

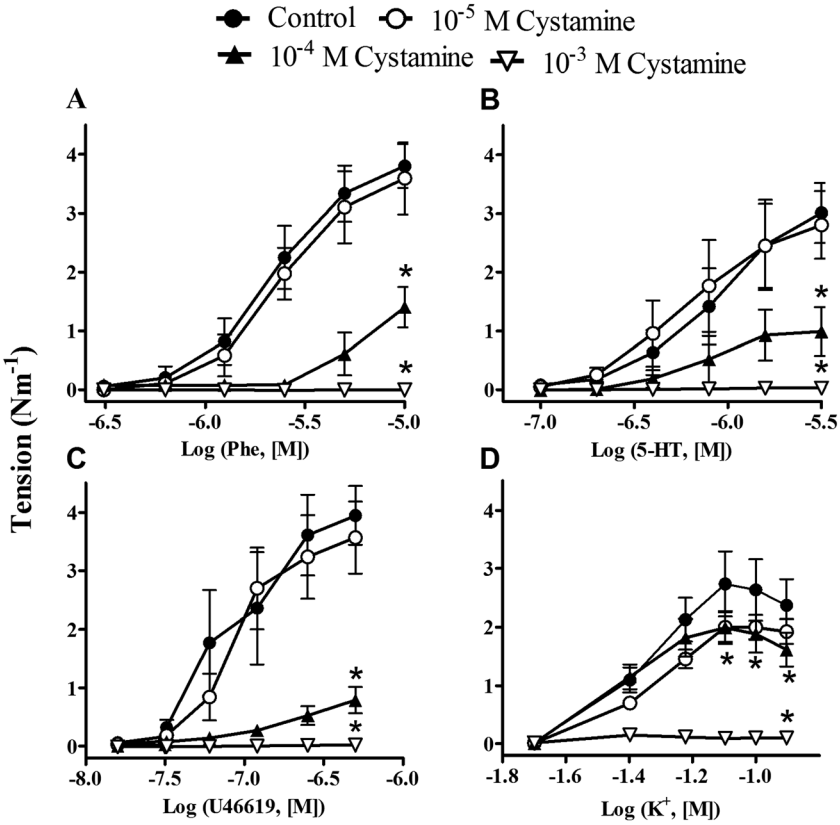

Figure 2

Effect of cystamine on concentration–response curves for phenylephrine; 5-HT; the TxA_2 analogue, U46619; and extracellular potassium (K^+). Rat mesenteric small arteries (diameter <300 μm) were incubated with vehicle or different concentrations of cystamine (10^{-5}–10^{-3} M). Results are means ± SEM, vessel segments from six rats. Differences were evaluated by repeated measures of ANOVA followed by a Bonferroni post test. *$P < 0.05$.

Effect of cystamine on agonist and KPSS contraction

Cystamine (10^{-5}–10^{-4} M) inhibited the concentration–response curves for phenylephrine, 5-HT and the TxA_2 receptor agonist U46619 (Figure 2A–C; Supporting Information Table 1), while only the maximum response to increasing concentrations of extracellular potassium was reduced (Figure 2D). A high concentration of cystamine (1 mM) abolished the contractions induced by all receptor agonists, and also to KPSS (Figure 2), and although the effect of 1 mM cystamine was reversible after 2 h with exchange of the bath solution with 10 min intervals, the concentration is far above the plasma thiol concentrations measured in rats treated with cystamine (Engholm *et al.*, 2011) and was therefore not investigated further.

Effect of PLC and TG2 inhibition in rat mesenteric arteries

Cystamine has been reported to cause inhibition of other transglutaminases, and therefore, the effect of other TG2 inhibitors was examined (Figure 3). Monodansylcadaverine and also the cell-impermeable TG2 inhibitor T101 induced relaxations with comparable potency and magnitude as cystamine, while a cell-permeable TG2 inhibitor, LDN 27219, was more potent than the other compounds (Figure 3B). Monodansylcadaverine binds to the catalytic site, and pretreatment of the preparations with monodansylcadaverine caused significant inhibition of cystamine and LDN 27219 relaxation in rat mesenteric arteries (Figure 3A, C, D), while relaxations induced by U73122, a PLC inhibitor, were unaltered in the presence of monodansylcadaverine (Figure 3A, E).

To investigate whether cystamine relaxation involves PLC, preparations were incubated with the PLC inhibitor, U73122. U73122 (10 μM) induced pronounced inhibition of phenylephrine contraction, and therefore, the concentration of the inhibitor was lowered to 5 μM, and by adding additional phenylephrine, 50% of the contraction was preserved (Figure 4). In these conditions, cystamine relaxation was inhibited, while the inactive analogue, U73343 (10 μM), failed to change cystamine relaxation (Figure 4).

Effects of cystamine on smooth muscle calcium

The concentration-dependent effects of cystamine on calcium responses to phenylephrine and high potassium were

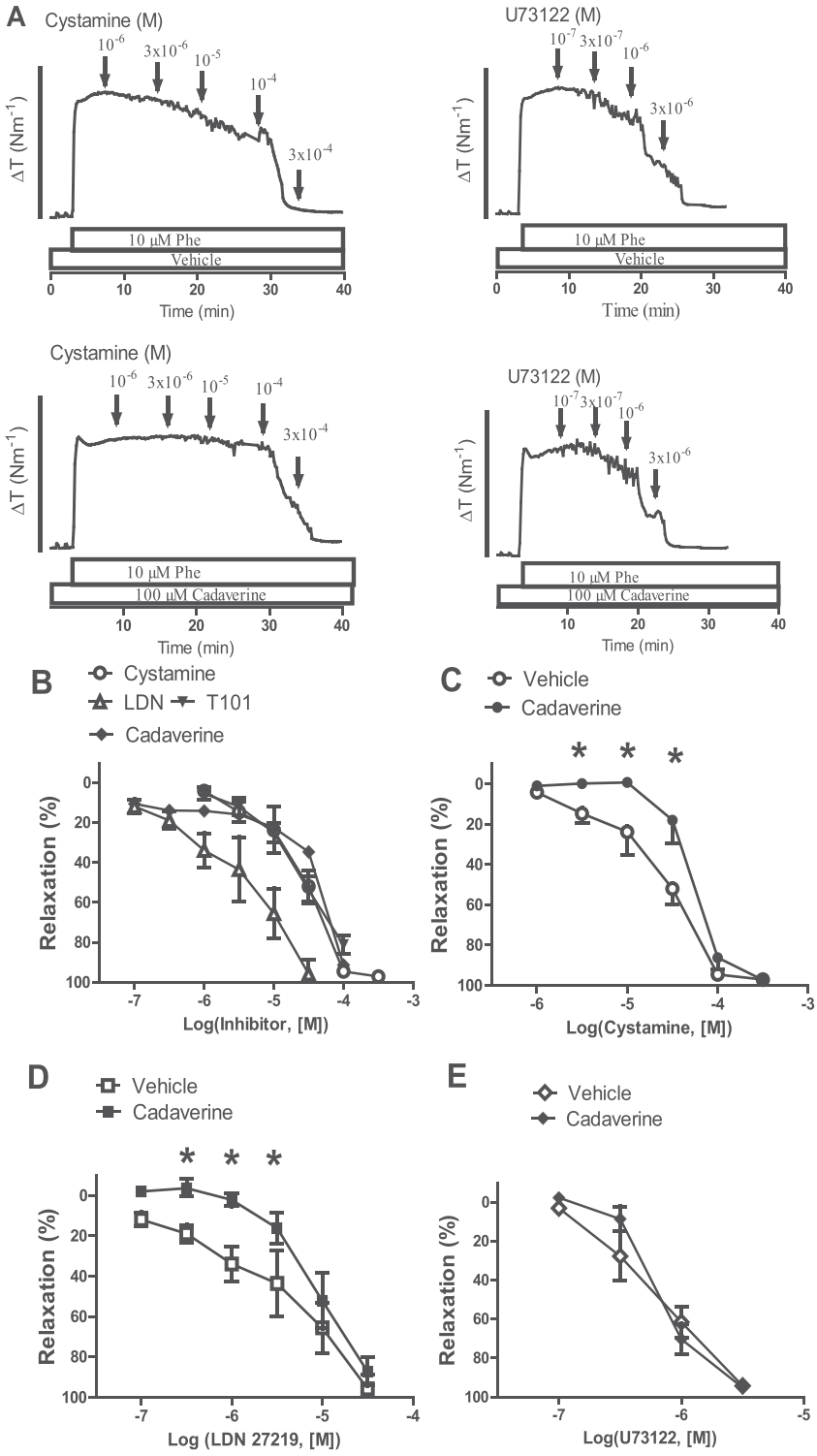

Figure 3

TG2 involved in cystamine relaxation of mesenteric small arteries. (A) Original traces showing contraction to phenylephrine (Phe; 10 μM) in preparations pretreated with either vehicle or the inhibitor of TG2, monodansylcadaverine, followed by concentration–response curves for either cystamine or the PLC inhibitor, U73122. The bar corresponds to a tension (ΔT) of 4 Nm^{-1}. (B) Average concentration–response curves for cystamine, a TG2 selective non-cell-permeable inhibitor, T101; a TG2 selective cell-permeable inhibitor, LDN 27219; and the suicide substrate, monodansylcadaverine, in arteries contracted with phenylephrine. Arteries were incubated with monodansylcadaverine (100 μM) followed by a washout and then construction of concentration–response curves for (C) cystamine, (D) LDN 27219 or (E) a phospholipase inhibitor, U73122. Monodansylcadaverine pretreatment caused significant rightward shifts in the concentration–response curves for cystamine and LDN 27219. *$P < 0.05$ versus the control curve (vehicle), $n = 6$.

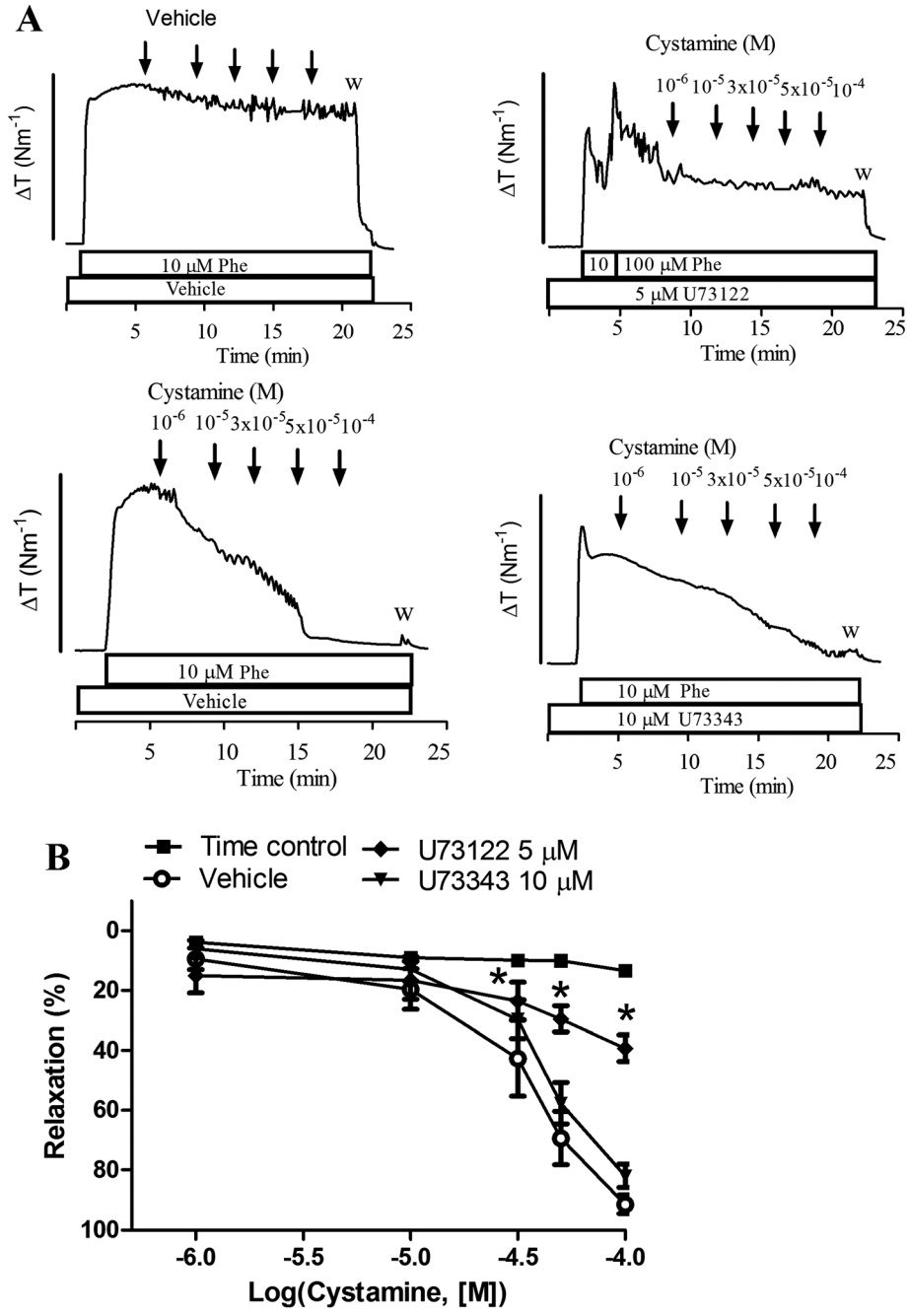

Figure 4

Phospholipase C inhibitor blunts cystamine relaxation in mesenteric small arteries. (A) Original traces showing contraction to phenylephrine (Phe; 10 μM) in preparations where vehicle was added (time control) or incubated with vehicle, an inhibitor of PLC, U73122 (5 μM), or the inactive analogue, U73343 (10 μM), followed by concentration–response curves for cystamine. The bar corresponds to a tension (ΔT) of 4 Nm^{-1}. (B) Average concentration–response curves for cystamine obtained in the absence (vehicle) and presence of U73122 or U73343. *$P < 0.05$ versus the curve obtained in the presence of vehicle, $n = 6$.

then determined (Figures 5 and 6). Cystamine caused a concentration-dependent inhibition of calcium and contraction to phenylephrine (Figure 5).

Depolarization with 100 mM KPSS caused contraction and an increase in $[Ca^{2+}]_i$ (Figure 6). When cystamine (100 μM) was added, there was a gradual reduction of tension, while $[Ca^{2+}]_i$ was unchanged (Figure 6).

Role of endothelium and K^+ channels in cystamine relaxation of rat mesenteric arteries

Cystamine induced comparable relaxations in mesenteric arteries with and without endothelium (Supporting Information Figure 1), but less relaxation in preparations activated with KPSS. Therefore, it was investigated whether K^+ channels are involved in cystamine relaxations (Figure 7). Glibenclamide

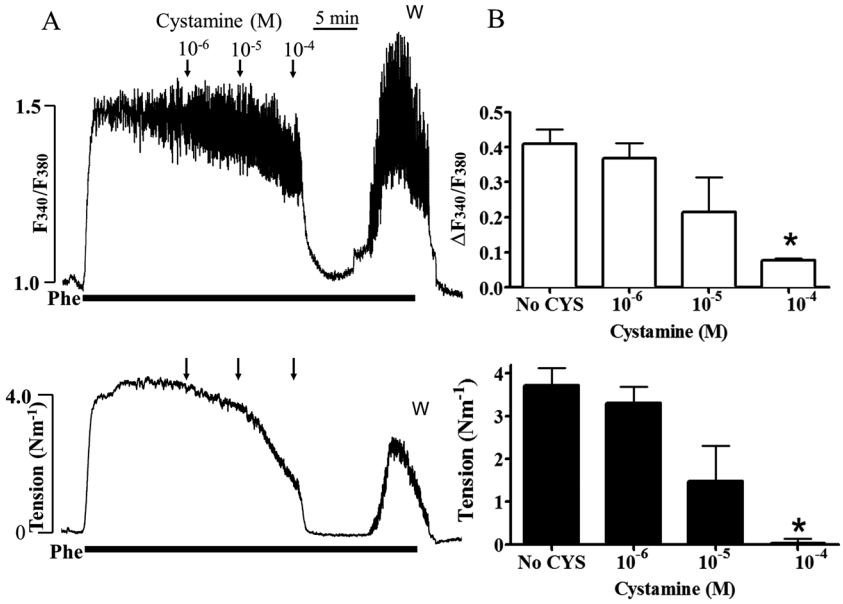

Figure 5

Effect of cystamine (CYS) on calcium and tension in rat mesenteric arteries contracted with phenylephrine. (A) Original traces of Fura-2AM ratio ($\Delta F_{340}/F_{380}$) as a measure of change in $[Ca^{2+}]_i$ and tension of rat mesenteric small artery in response to 10 μM phenylephrine (Phe), followed by addition of increasing concentrations of cystamine. Cystamine 100 μM caused acute reduction in active tension and F_{340}/F_{380}. This inhibition persisted for about 10 min after which an increase in F_{340}/F_{380} was observed together with a rise in tension. (B) Average changes in Fura-2 ratio and tension. *$P < 0.05$ versus initial response.

(1 μM), TEA (1 mM) and 4-aminopyridine failed to change cystamine relaxation (Figure 7), but glibenclamide caused marked inhibition of relaxations induced by an opener of ATP-sensitive K^+ channels, levcromakalim (Supporting Information Figure 2A), and TEA of relaxations induced by an opener of large-conductance calcium-activated and K_v7 channels, NS11021 (Supporting Information Figure 2B). Blockers of the voltage-gated K_v7 channels, XE991 and linopirdine, caused inhibition of cystamine relaxation (Figure 7D, E) and of relaxations induced by NS11021 (Supporting Information Figure 2B) and did not change relaxations induced by SNP (results not shown, $n = 6$).

Whole-cell patch clamp

Further evidence for the importance of K_v7 channels in cystamine relaxations was obtained from voltage clamp experiments. Representative families of K_v currents in smooth muscle cells isolated from rat mesenteric arteries were evoked by voltage steps between −95 and +45 mV (Figure 8, Supporting Information Figure 3), and these were markedly enhanced by cystamine (10^{-4} M). Both XE991 and linopirdine inhibited the cystamine-induced currents (Figure 8C, D).

Effect of cystamine on ratios of p-MYPT1/MYPT1 and p-MLC/MLC

To assess the involvement of the kinase ROCK in the Ca^{2+} desensitization, we analysed ROCK activity by measuring the phosphorylation of MYPT1 using a primary antibody against p-MYPT1-Thr^{855}. Average expression of MYPT1 and MLC2 was similar across the different treatments, and therefore, the phosphorylated proteins were expressed as ratio to total MYPT1 and MLC respectively. The peak in p-MYPT1/MYPT1 ratio following stimulation with 10 μM phenylephrine was maximal between 1 and 2 min following activation with phenylephrine (Supporting Information Figure 4A). The mechanism for this increase was then investigated in a series of experiments (Figure 9). Cystamine significantly ($P < 0.05$) reduced the basal level of phosphorylated MYPT1. The numeric reduction in p-MYPT1/MYPT1 ratio induced by cystamine was not significant in the absence and presence of phenylephrine ($P = 0.72$, $n = 12$) despite a significant reduction of phenylephrine contraction (Figure 9). Y27632 (1 μM), a selective inhibitor of ROCK, almost eliminated the baseline level of phosphorylated MYPT1 ($P < 0.01$) and also reduced the phosphorylation of MYPT1 induced by phenylephrine ($P < 0.001$) although without altering tone. In 100 mM KPSS-contracted arteries, MYPT1 phosphorylation remained unaltered by addition of cystamine (Supporting Information Figure 4B).

Phenylephrine markedly increased the p-MLC2/MLC2 ratio (Figure 9). In contrast to Y27632, cystamine failed to change p-MLC2/MLC2 ratio in vessels activated with both phenylephrine (Figure 9) and 100 mM KPSS (Supporting Information Figure 4B).

Effect of tempol, rotenone and antimycin on cystamine relaxation

To investigate cystamine relaxations persisting despite the presence of a high extracellular potassium, the preparations were incubated with inhibitors of mitochondrial complexes I and III, respectively, rotenone (1 μM) and antimycin A

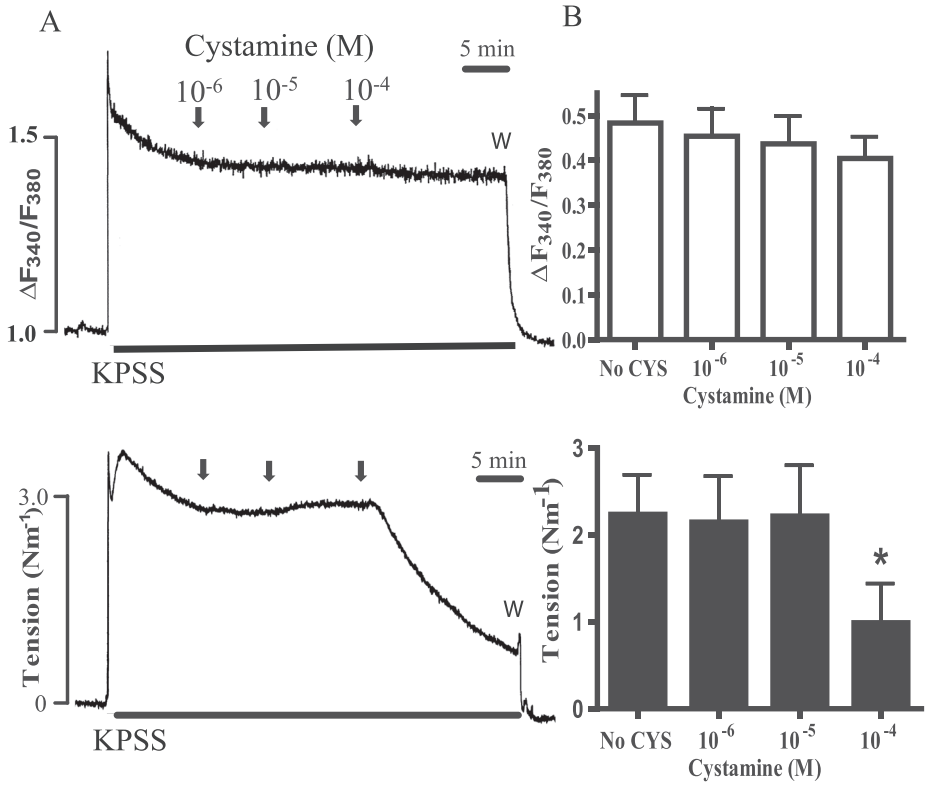

Figure 6

Effect of cystamine (CYS) on calcium and tension in rat mesenteric arteries contracted with high extracellular potassium. (A) Original traces of Fura-2AM ratio ($\Delta F_{340}/F_{380}$) as a measure of change in $[Ca^{2+}]_i$ and tension of rat mesenteric small artery in response to high extracellular potassium (KPSS) applied in combination with 1 μM phentolamine, to minimize stimulated release of neuronal noradrenaline. Once KPSS contraction was stable, increasing concentrations of cystamine were added. Active tension was reduced following the addition of cystamine 100 μM, but with no change in F_{340}/F_{380} ratio. (B) Average changes in Fura-2 ratio and tension. *$P < 0.05$ versus initial response.

(1 μM). Despite lower contraction in the presence of rotenone and antimycin A (Supporting Information Figure 5), both rotenone and antimycin A caused pronounced inhibition of cystamine relaxation (Figure 10A, B), while SNP relaxation was only reduced marginally by rotenone (Figure 10C). The superoxide scavengers, tempol and mito-tempo, failed to change cystamine and SNP relaxation (Figure 10D, E).

Discussion

The purpose of this study was to investigate the mechanisms for the vasoactive effects of cystamine in rat mesenteric small arteries. The findings that selective inhibitors of TG2 have the same effect as cystamine and that mainly TG2 is expressed in rat mesenteric small arteries support the suggestion that vascular effects of cystamine are induced by inhibition of TG2. Furthermore, in phenylephrine-activated vessels, 100 μM cystamine caused simultaneous reduction in both $[Ca^{2+}]_i$ and tension, and blockers of K_V7 channels, XE991 and linopirdine, reduced both the relaxations and the increase in smooth muscle current induced by cystamine. In vessels activated with high extracellular potassium, 100 μM cystamine reduced tension without altering $[Ca^{2+}]_i$. Cystamine did not affect the level of phosphorylated MYPT1 and MLC2 in phenylephrine and potassium-activated vessels, but cystamine relaxations in potassium-activated arteries were sensitive to inhibitors of mitochondrial complexes I and III. These findings raise the possibility that 100 μM cystamine in addition to leading to opening of K_V7 channels may cause force suppression by a mechanism leading to uncoupling of the mitochondrial respiratory chain.

In previous studies, we demonstrated TG2 protein expression in mesenteric small arteries (Eftekhari *et al.*, 2007), but recently, TG1 and TG4 were also found to be expressed in rat aorta and vena cava (Johnson *et al.*, 2012). Our RT-PCR studies showed a marked expression of TG2 and a weak band for TG1 mRNA. Cystamine is an inhibitor of transglutaminases with some selectivity towards TG2 (Jeitner *et al.*, 2005; Schaertl *et al.*, 2010), but at concentrations above 100 μM, cystamine may also inhibit TG1 (Jeitner *et al.*, 2005). Although TG1 expression was not detected by immunoblotting, we cannot exclude the possibility that inhibition of TG1 or other mechanisms may contribute to the relaxations induced by high concentrations of cystamine in the present study.

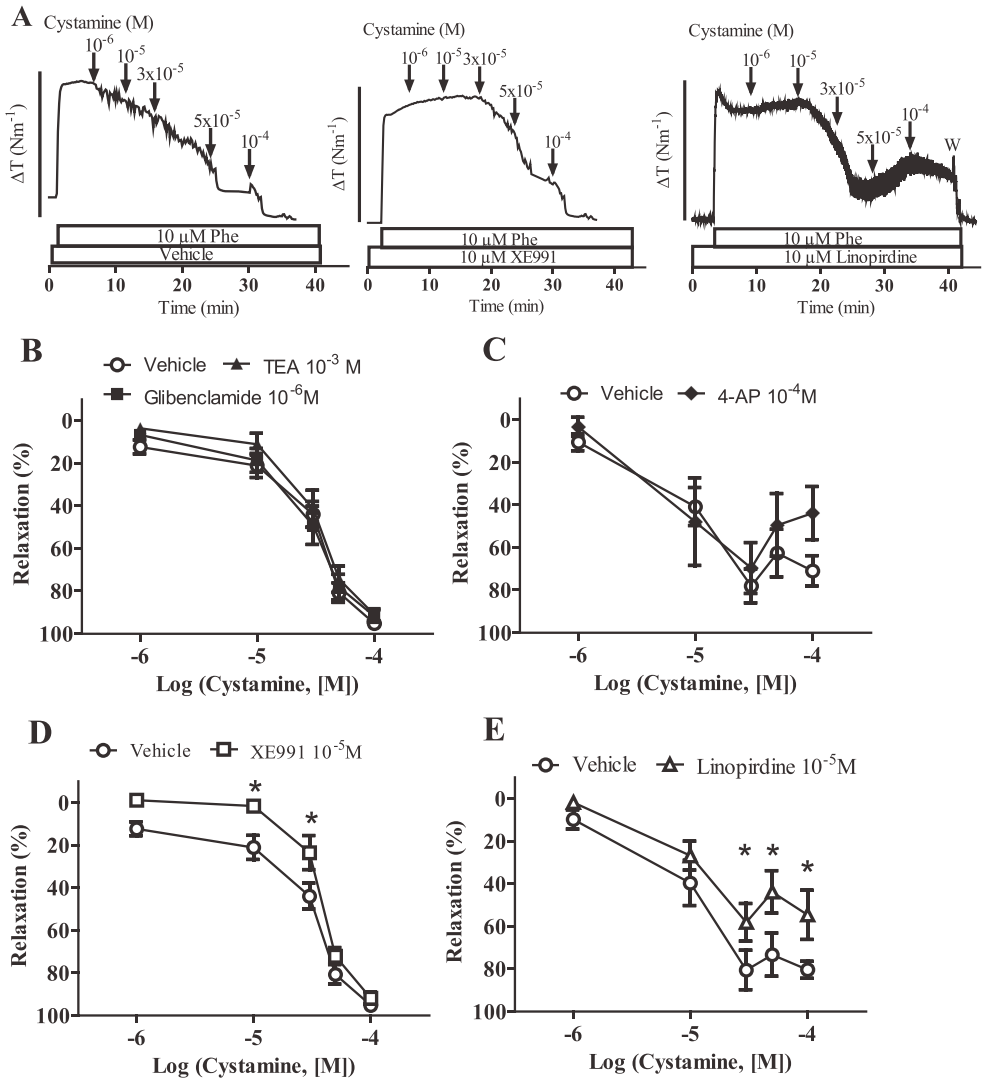

Figure 7

XE991-sensitive K^+ channels are involved in cystamine relaxation. (A) Original traces showing contraction to phenylephrine (Phe; 10 µM) in preparations incubated with vehicle or blockers of K_v7 channels, XE991 (10 µM) and linopirdine (10 µM) followed by concentration–response curves for cystamine. The bar corresponds to a tension (ΔT) of 4 Nm^{-1}. Average concentration–response curves for cystamine in the absence [vehicle, n = 7 (B, D) and n = 11 (C, E)] and (B) presence of a blocker of ATP-sensitive K^+ channels, glibenclamide (10^{-6} M, n = 7), or a blocker of calcium-activated K^+ channels, TEA (1 mM, n = 7), and (C) in the presence of 4-aminopyridine (4-AP; 0.5 mM, n = 6), (D) XE991 (10 µM, n = 7) and (E) linopirdine (10 µM, n = 8). *$P < 0.05$ versus the curve obtained in the presence of vehicle; two-way ANOVA followed by Bonferroni t-test.

Cystamine has previously been found to decrease contractions induced by 5-HT in canine coronary arteries and rat aorta (Fujioka *et al.*, 1993; Watts *et al.*, 2009) and by phenylephrine in rat mesenteric arteries (Eftekhari *et al.*, 2007) as well as in human myometrium (Alcock *et al.*, 2011). Moreover, cystamine inhibition of contraction was independent of the presence of the endothelium in dog coronary arteries. Thus, our findings that cystamine reduces agonist-induced contraction in a concentration-dependent manner and independent of the endothelium are consistent with previous findings.

TG2 is expressed both intracellularly and at the surface of vascular smooth muscle cells in rat mesenteric arteries, and activity assays suggest that both intracellular and extracellular transglutaminases are active in the presence of calcium (Eftekhari *et al.*, 2007; van den Akker *et al.*, 2011). Moreover, it has been argued that extracellular TG2 could be activated by mechanical force within the vascular wall (Huelsz-Prince *et al.*, 2013). To clarify whether intracellular or extracellular transglutaminase contributes to cystamine relaxation, a cell-impermeable TG2 inhibitor, T101 (Antonyak *et al.*, 2011), was added and produced relaxations that were similar in potency and magnitude to those induced by cystamine. The cell-permeable and TG2 selective inhibitor, LDN 27219 (Case and Stein, 2007), caused pronounced relaxations of rat mesenteric arteries. That these relaxations can be ascribed to inhibition of transglutaminases was confirmed by the observation that incubation with monodansylcadaverine

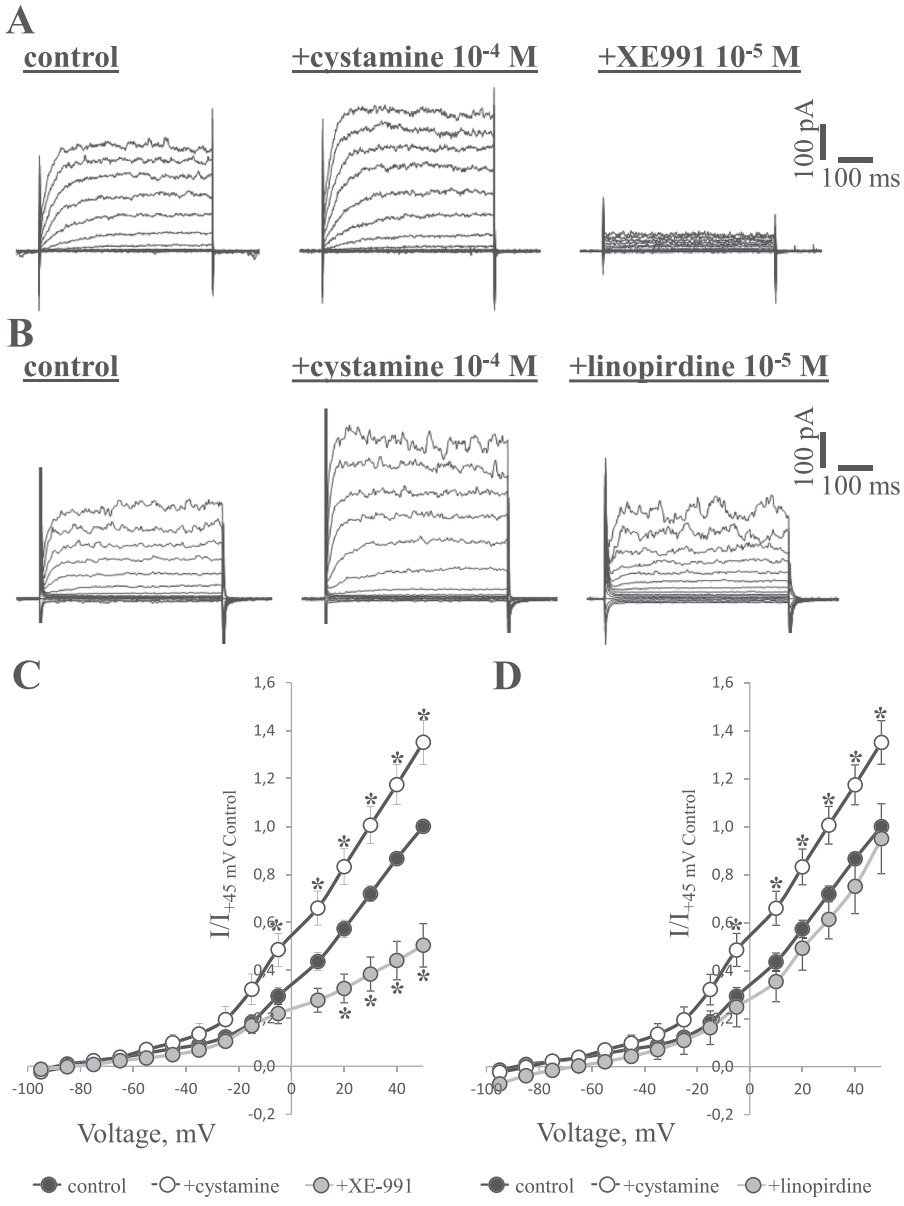

Figure 8

Cystamine activates Kv current in smooth muscle cells isolated from rat mesenteric arteries. (A) Representative families of Kv currents in smooth muscle cells isolated from rat mesenteric arteries evoked by voltage steps between −95 and +45 mV. The recordings were made under control conditions, after the application of 10^{-4} M cystamine and then following application of 10^{-5} M XE991, as indicated. (B) Representative families of Kv currents in smooth muscle cells isolated from rat mesenteric arteries evoked by voltage steps between −95 and +45 mV. Experiment similar to A, but after the application of 10^{-4} M cystamine, 10^{-5} M linopirdine was applied. (C) Averaged I–V relations for Kv currents from the experiments shown in A (n = 11). (D) Averaged I–V relations for Kv currents from the experiments shown in B (n = 5). *$P < 0.05$ versus control.

inhibited both cystamine and LDN 27219-induced relaxations. These findings suggest that both intracellular and extracellular transglutaminases contribute to cystamine relaxations in rat mesenteric arteries.

In cardiovascular cells, TG2 is involved in transmembrane signalling as a G-protein (G_h) transmitting signals from seven-transmembrane receptors, including α_{1b} and α_{1d} adrenoceptors, Tx and oxytocin receptors, to PLC (Fesus and Piacentini, 2002). The inhibition of agonist-induced vasoconstriction by cystamine could possibly involve competitive inhibition of TG2/G_h-coupled/catalysed signalling pathways and, thus, inhibition of signal transmission and PLC activation. In the present study, an inhibitor of PLC, U73122, blunted cystamine relaxations. This effect appears to be specific as an inactive analogue, U73343, failed to change cystamine relaxations. Although our evidence is indirect and based on adjusting the phenylephrine contraction, these findings suggest that at least part of the relaxant effect

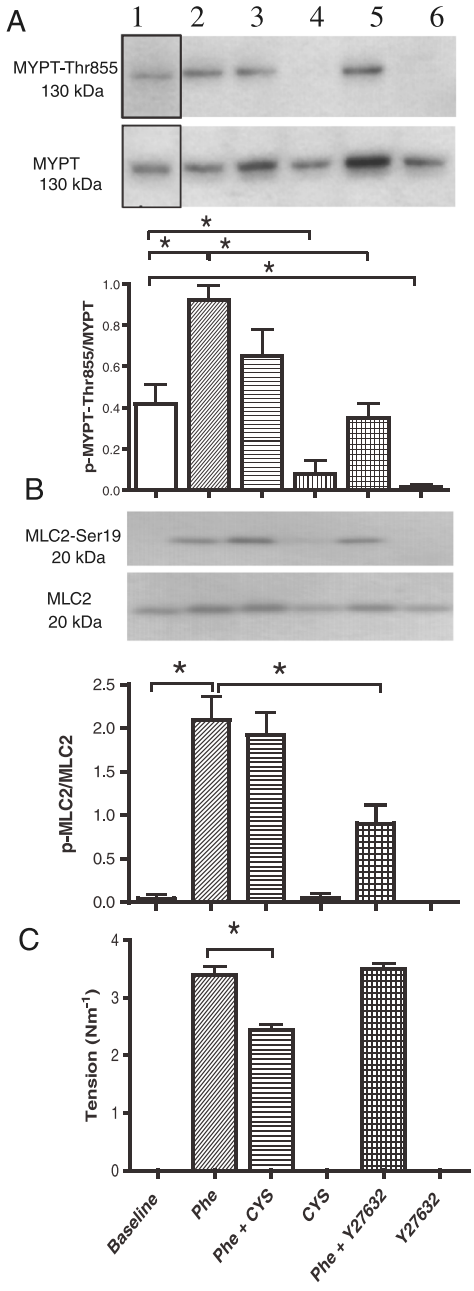

Figure 9

Simultaneous measurements of (A) phosphorylation of myosin phosphatase targeting subunit 1 (MYPT1-Thr^{855}), of (B) phosphorylation of regulatory myosin light chain (MLC2-Ser^{19}) and of (C) tension in rat mesenteric arteries. Arterial segments were exposed to phenylephrine (Phe; 10 μM), cystamine (100 μM), KPSS (100 mM) or Y27632 (1 μM) alone or in combination. Once tension was measured, the preparations were snap-frozen for immunoblotting for p-MYPT- Thr^{855} and for MYPT. (B) Ratio of p-MYPT1/MYPT1. Cystamine reduced the tension and basal phosphorylation of MYPT1 (p-MYPT1/MYPT1), while phenylephrine-induced increase in phosphorylation was unaltered. The ROCK inhibitor, Y27632 (1 μM), reduced both phenylephrine and basal p-MYPT1/MYPT1. (C) Abscissae show wall tension and p-MLC2-Ser^{19}/MLC2 ratio determined by Western blot in vessels mounted on wire myograph. Data are means ± SEM of vessel segments from 14 animals. *$P < 0.05$, ANOVA.

of cystamine can be ascribed to an effect on transglutaminase upstream from PLC. Transglutaminase has indeed been suggested to be involved in dimerization (Yamada *et al.*, 2008) and prevention of angiotensin AT_1 receptor ubiquitination–protein degradation (Liu *et al.*, 2014) as well as in AT_2 receptor oligomerization in a mouse model of Alzheimer's disease (AbdAlla *et al.*, 2009), but other approaches are required to clarify whether transglutaminases contribute to stabilization of other G-protein-coupled receptors including the α_1-adrenoceptors.

Our findings that cystamine (1–100 μM) had less effect on potassium-evoked contraction than on agonist-evoked contractions would be consistent with the opening of K^+ channels (Jackson, 2000). Furthermore, cystamine (10–100 μM) lowered calcium in phenylephrine-contracted preparations, while this was not the case in potassium-contracted preparations. Investigation of several K^+ channel blockers revealed that blockers of K_v7 channels, XE991 and linopirdine, inhibited cystamine relaxations. These findings suggest that K_v7 channels are involved in cystamine relaxations of mesenteric arteries. K_v7 channels ($K_v7.1$, $K_v7.4$ and K_v7 5) are expressed in rat mesenteric arteries, and activation of these channels leads to vasodilatation (Mackie *et al.*, 2008; Jepps *et al.*, 2011). In agreement with the previous studies, a XE991-sensitive current was detected in rat mesenteric smooth muscle, and cystamine was found to increase the current. TEA with IC_{50} values of 3–5 mM was found to block K_v7 channels expressed in CHO cells (Hadley *et al.*, 2000), but only 1 mM TEA, which mainly blocks large-conductance calcium-activated K^+ channels, was used in the present study. XE991 can also attenuate $K_v1.2/K_v1.5$ and $K_v2.1/K_v9.3$ channels (Zhong *et al.*, 2010), and high extracellular potassium had a more pronounced inhibitory effect on cystamine relaxation than XE991 and linopirdine. Therefore, other approaches, for example, perforated patch configuration, will be required to further delineate whether other K_v channel subtypes are involved (Brueggemann *et al.*, 2012), but our present findings that both XE991 and linopirdine inhibit cystamine-induced relaxation and increase in current suggest that K_v7 channels contribute to cystamine-induced relaxation in rat mesenteric arteries.

In K^+-contracted arteries, 100 μM cystamine still caused relaxation without changes in $[Ca^{2+}]_i$, suggesting that cystamine causes Ca^{2+} desensitization by affecting MLC-Ser^{19} phosphorylation, MLCP activity or force suppression, which occurs when force is reduced despite persistent elevation in MLC-Ser^{19} phosphorylation levels (Rembold, 2007). Inhibition of MLCP can occur either directly by phosphorylation of MYPT1, for instance, by ROCK or indirectly via phosphorylation of CPI-17 by PKC (Somlyo and Somlyo, 2003). In the present study, cystamine and Y27632 lowered MYPT-Thr^{855} phosphorylation at baseline, suggesting that TG2 may play a role for ROCK activation in rat mesenteric arteries. In phenylephrine-activated arteries, our simultaneous measurements of tension and MYPT-Thr^{855}phosphorylation revealed that contractility in these small arteries is independent of ROCK. Thus, despite reduced MYPT-Thr^{855} phosphorylation, Y27632 failed to change phenylephrine-induced contractions, and cystamine reduced the tension without changes in MYPT-Thr^{855} phosphorylation. These findings are consistent with

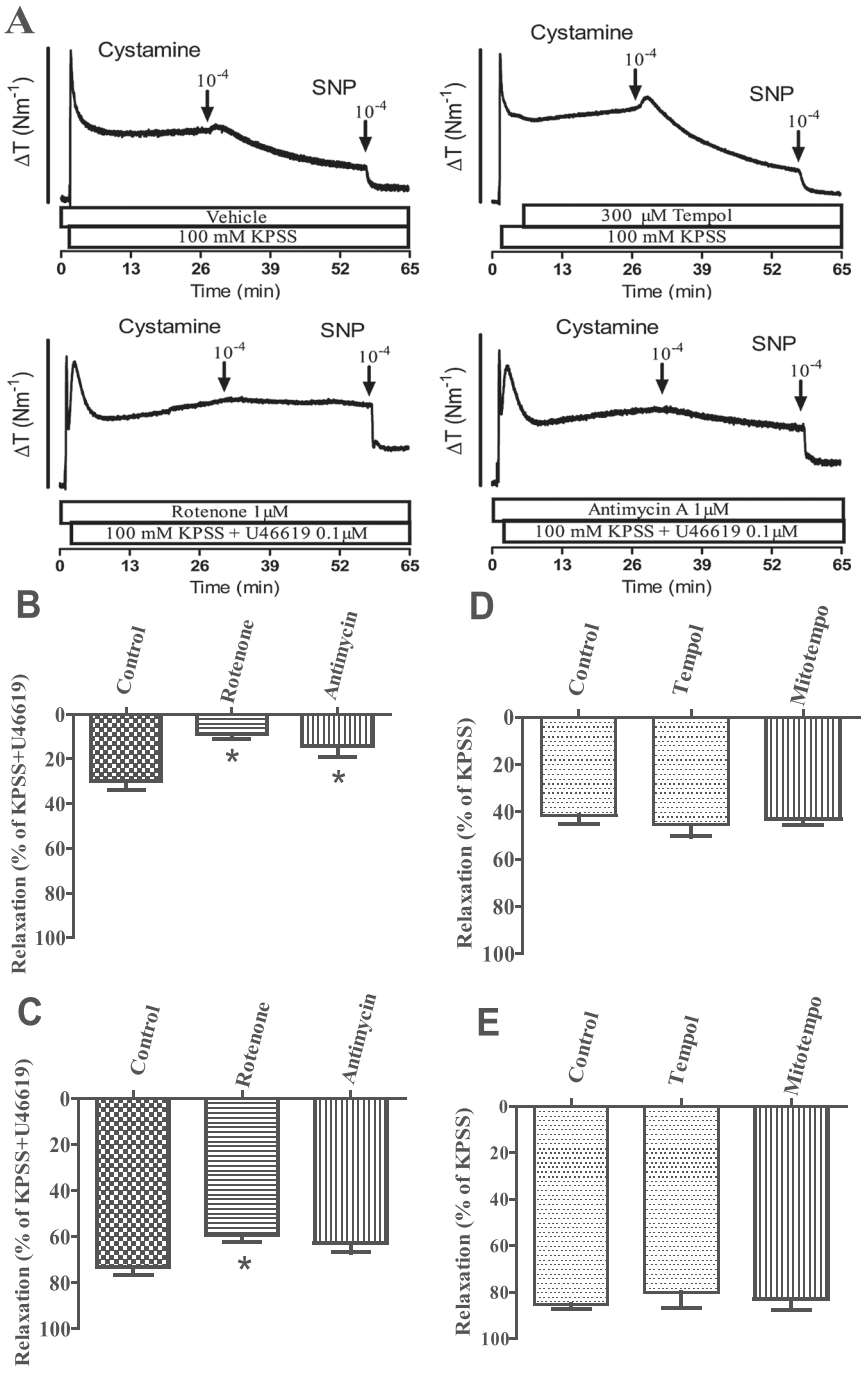

Figure 10

Inhibitors of mitochondrial complexes I and III block cystamine relaxation in rat mesenteric arteries. (A) Original recordings showing contractions induced by extracellular KPSS (100 mM) in the presence of vehicle, a superoxide scavenger, tempol, and an inhibitor of complex I, rotenone, and of complex III, antimycin, followed by addition of cystamine and the NO donor, SNP. U46619 was added to increase contraction in preparations incubated with rotenone and antimycin. The bar corresponds to a tension (ΔT) of 4 Nm^{-1} in the upper traces and of 3 Nm^{-1} in the lower traces. (B–E) Average relaxation induced by (B, D) cystamine (10^{-4} M) or (C, E) SNP in preparations incubated with rotenone, antimycin, tempol or the mitochondrial superoxide scavenger, mito-tempo, in preparations contracted with (D, E) KPSS or in case the incubation affected the contraction level by (B,C) KPSS plus U46619. Data are means ± SEM of vessel segments from 10 animals. *$P < 0.05$ versus control.

the findings by Budzyn *et al.* (2006, who report that contractile responses of mesenteric small arteries seem to be mediated exclusively by PKC, with no role for ROCK. This suggests that the Ca^{2+} desensitization observed with cystamine may be mediated through interaction with PKC-associated phosphorylation of CPI-17 and hence inhibition of MLCP-activity

(Eto *et al.*, 1997) but is less likely, because the reduction in force with cystamine was not associated with a significant reduction in the phosphorylation of MLC (Figure 9).

Mice deficient in TG2 have previously been suggested to be associated with reduced activity of mitochondrial complex I (Mastroberardino *et al.*, 2006). Inhibition of the mitochondrial complexes has been suggested to involve formation of free radicals including superoxide (Dikalova *et al.*, 2010), but in our experiments, incubation with the superoxide mimetic tempol or mitochondria-specific superoxide mimetic, mito-tempo, failed to change cystamine relaxation. However, inhibition of respectively mitochondrial complexes I and III, with rotenone and antimycin A, blocked cystamine relaxation persisting in the presence of high extracellular potassium. Although further investigation will be required to reveal the underlying mechanism, deficiency of TG2 was associated with a glycolytic shift and low ATP content (Battaglia *et al.*, 2007), and therefore, inhibition of TG2 by cystamine may lead to reduced actin–MLC cross-bridge turnover (Han *et al.*, 2006) or to an increased smooth muscle AMP-to-ATP ratio followed by activation of AMP kinase and vasodilatation (Rubin *et al.*, 2005). The protein disulphide isomerase activity of mitochondrial TG2 affecting complex I has been suggested to be involved in neurodegenerative disease (Rossin *et al.*, 2015), and therefore, inhibition by cystamine of both mitochondrial TG2 and TG2 proximal to PLC in the membrane leading to opening of K_v channels and vasodilatation may contribute to the neuroprotective and antihypertensive effect of cystamine.

In conclusion, our findings suggest that cystamine induced vasodilatation in rat mesenteric small arteries by inhibition of receptor-coupled TG2, leading to opening of K_v channels and reduction of intracellular calcium as well as activation of a pathway sensitive to inhibitors of the mitochondrial complexes I and III. Both pathways may contribute to the antihypertensive and neuroprotective effect of cystamine.

Acknowledgements

This project was supported by the Danish Medical Research Council, the Danish Heart Foundation and the Novo Nordisk Foundation. The authors would like to thank Henriette Johansson for technical assistance.

Author Contributions

M. E. participated in designing and performing the experiments and wrote a first draft of the manuscript. E. P. performed and analysed the experiments with K channel blockers, mitochondrial inhibitors and patch clamp. S. M. designed and performed the RT-PCR experiments, reported the sequences to NCBI and wrote the corresponding parts. V. V. M. designed and performed the voltage clamp experiments and wrote the corresponding parts. E. R. H. designed and performed the immunoblotting experiments and contributed to the writing. H. C. performed the experiments in vessels with and without endothelium and wrote the corresponding parts. M. M. participated in designing and analysing the experiments as well as writing. U. S. participated in designing and analysing the experiments and wrote in part the manuscript.

Conflict of interest

There are no conflicts of interest.

References

AbdAlla S, Lother H, el Missiry A, Langer A, Sergeev P, el Faramawy Y, *et al.* (2009). Angiotensin II AT2 receptor oligomers mediate G-protein dysfunction in an animal model of Alzheimer disease. J Biol Chem 284: 6554–6565.

Alcock J, Warren AY, Goodson YJ, Hill SJ, Khan RN, Lymn JS (2011). Inhibition of tissue transglutaminase 2 attenuates contractility of pregnant human myometrium. Biol Reprod 84: 646–653.

Alexander SPH, Catterall WA, Kelly E, Marrion N, Peters JA, Benson HE, *et al.* (2015a). The Concise Guide to PHARMACOLOGY 2015/16: Voltage-gated ion channels. Br J Pharmacol 172: 5904–5941.

Alexander SPH, Fabbro D, Kelly E, Marrion N, Peters JA, Benson HE, *et al.* (2015b). The Concise Guide to PHARMACOLOGY 2015/16: Enzymes. Br J Pharmacol 172: 6024–6109.

Antonyak MA, Li B, Boroughs LK, Johnson JL, Druso JE, Bryant KL, *et al.* (2011). Cancer cell-derived microvesicles induce transformation by transferring tissue transglutaminase and fibronectin to recipient cells. Proc Natl Acad Sci U S A 108: 4852–4857.

Bakker EN, Buus CL, Spaan JA, Perree J, Ganga A, Rolf TM, *et al.* (2005). Small artery remodeling depends on tissue-type transglutaminase. Circ Res 96: 119–126.

Battaglia G, Farrace MG, Mastroberardino PG, Viti I, Fimia GM, Van BJ, *et al.* (2007). Transglutaminase 2 ablation leads to defective function of mitochondrial respiratory complex I affecting neuronal vulnerability in experimental models of extrapyramidal disorders. J Neurochem 100: 36–49.

Budzyn K, Paull M, Marley PD, Sobey CG (2006). Segmental differences in the roles of rho-kinase and protein kinase C in mediating vasoconstriction. J Pharmacol Exp Ther 317: 791–796.

Brueggemann LI, Mani BK, Haick J, Byron KL (2012). Exploring arterial smooth muscle Kv7 potassium channel function using patch clamp electrophysiology and pressure myography. J Vis Exp 67: e4263.

Buus CL, Aalkjaer C, Nilsson H, Juul B, Moller JV, Mulvany MJ (1998). Mechanisms of Ca2+ sensitization of force production by noradrenaline in rat mesenteric small arteries. J Physiol 510 (Pt 2): 577–590.

Case A, Stein RL (2007). Kinetic analysis of the interaction of tissue transglutaminase with a nonpeptidic slow-binding inhibitor. Biochemistry 46: 1106–1115.

Dedeoglu A, Kubilus JK, Jeitner TM, Matson SA, Bogdanov M, Kowall NW, *et al.* (2002). Therapeutic effects of cystamine in a murine model of Huntington's disease. J Neurosci 22: 8942–8950.

Dikalova AE, Bikineyeva AT, Budzyn K, Nazarewicz RR, McCann L, Lewis W, *et al.* (2010). Therapeutic targeting of mitochondrial superoxide in hypertension. Circ Res 107: 106–116.

Eftekhari A, Rahman A, Schaebel LH, Chen H, Rasmussen CV, Aalkjaer C, *et al*. (2007). Chronic cystamine treatment inhibits small artery remodelling in rats. J Vasc Res 44: 471–482.

Engholm M, Eftekhari A, Chwatko G, Bald E, Mulvany MJ (2011). Effect of cystamine on blood pressure and vascular characteristics in spontaneously hypertensive rats. J Vasc Res 48: 476–484.

Eto M (2009). Regulation of cellular protein phosphatase-1 (PP1) by phosphorylation of the CPI-17 family, C-kinase-activated PP1 inhibitors. J Biol Chem 284: 35273–35277.

Eto M, Senba S, Morita F, Yazawa M (1997). Molecular cloning of a novel phosphorylation-dependent inhibitory protein of protein phosphatase-1 (CPI17) in smooth muscle: its specific localization in smooth muscle. FEBS Lett 410: 356–360.

Fesus L, Piacentini M (2002). Transglutaminase 2: an enigmatic enzyme with diverse functions. Trends Biochem Sci 27: 534–539.

Fujioka H, Horiike K, Takahashi M, Ishida T, Kinoshita M, Nozaki M (1993). Triphasic vascular effects of thiol compounds and their oxidized forms on dog coronary arteries. Experientia 49: 47–50.

Gibrat C, Bousquet M, Saint-Pierre M, Levesque D, Calon F, Rouillard C, *et al*. (2010). Cystamine prevents MPTP-induced toxicity in young adult mice via the up-regulation of the brain-derived neurotrophic factor. Prog Neuro-Psychopharmacol Biol Psychiatry 34: 193–203.

Griffin M, Casadio R, Bergamini CM (2002). Transglutaminases: nature's biological glues. Biochem J 368: 377–396.

Hadley JK, Noda M, Selyanko AA, Wood IC, Abogadie FC, Brown DA (2000). Differential tetraethylammonium sensitivity of KCNQ1-4 potassium channels. Br J Pharmacol 129: 413–415.

Han S, Speich JE, Eddinger TJ, Berg KM, Miner AS, Call C, *et al*. (2006). Evidence for absence of latch-bridge formation in muscular saphenous arteries. Am J Physiol Heart Circ Physiol 291: H138–H146.

Hedegaard, ER, Mogensen, S & Simonsen, U. (2015). Rattus norvegicus strain Wistar transglutaminases mRNA, partial cds.

Hedegaard ER, Nielsen BD, Kun A, Hughes AD, Kroigaard C, Mogensen S, *et al*. (2014). KV 7 channels are involved in hypoxia-induced vasodilatation of porcine coronary arteries. Br J Pharmacol 171: 69–82.

Huelsz-Prince G, Belkin AM, VanBavel E, Bakker EN (2013). Activation of extracellular transglutaminase 2 by mechanical force in the arterial wall. J Vasc Res 50: 383–395.

Jackson WF (2000). Ion channels and vascular tone. Hypertension 35: 173–178.

Jeitner TM, Delikatny EJ, Ahlqvist J, Capper H, Cooper AJ (2005). Mechanism for the inhibition of transglutaminase 2 by cystamine. Biochem Pharmacol 69: 961–970.

Jepps TA, Chadha PS, Davis AJ, Harhun MI, Cockerill GW, Olesen SP, *et al*. (2011). Downregulation of Kv7.4 channel activity in primary and secondary hypertension. Circulation 124: 602–611.

Johnson KB, Petersen-Jones H, Thompson JM, Hitomi K, Itoh M, Bakker EN, *et al*. (2012). Vena cava and aortic smooth muscle cells express transglutaminases 1 and 4 in addition to transglutaminase 2. Am J Physiol Heart Circ Physiol 302: H1355–H1366.

Karpuj MV, Becher MW, Springer JE, Chabas D, Youssef S, Pedotti R, *et al*. (2002). Prolonged survival and decreased abnormal movements in transgenic model of Huntington disease, with administration of the transglutaminase inhibitor cystamine. Nat Med 8: 143–149.

Kun A, Matchkov VV, Stankevicius E, Nardi A, Hughes AD, Kirkeby HJ, *et al*. (2009). NS11021, a novel opener of large-conductance Ca(2+)-activated K(+) channels, enhances erectile responses in rats. Br J Pharmacol 158: 1465–1476.

Liu C, Wang W, Parchim N, Irani RA, Blackwell SC, Sibai B, *et al*. (2014). Tissue transglutaminase contributes to the pathogenesis of preeclampsia and stabilizes placental angiotensin receptor type 1 by ubiquitination-preventing isopeptide modification. Hypertension 63: 353–361.

Lorand L, Graham RM (2003). Transglutaminases: crosslinking enzymes with pleiotropic functions. Nat Rev Mol Cell Biol 4: 140–156.

Mackie AR, Brueggemann LI, Henderson KK, Shiels AJ, Cribbs LL, Scrogin KE, *et al*. (2008). Vascular KCNQ potassium channels as novel targets for the control of mesenteric artery constriction by vasopressin, based on studies in single cells, pressurized arteries, and in vivo measurements of mesenteric vascular resistance. J Pharmacol Exp Ther 325: 475–483.

Mastroberardino PG, Farrace MG, Viti I, Pavone F, Fimia GM, Melino G, *et al*. (2006). "Tissue" transglutaminase contributes to the formation of disulphide bridges in proteins of mitochondrial respiratory complexes. Biochim Biophys Acta 1757: 1357–1365.

McGrath JC, Lilley E (2015). Implementing guidelines on reporting research using animals (ARRIVE etc.): new requirements for publication in BJP. Br J Pharmacol 172: 3189–3193.

Mulvany MJ, Halpern W (1977). Contractile properties of small arterial resistance vessels in spontaneously hypertensive and normotensive rats. Circ Res 41: 19–26.

Pawson AJ, Sharman JL, Benson HE, Faccenda E, Alexander SPH, Buneman OP, *et al*. (2014). The IUPHAR/BPS Guide to PHARMACOLOGY: an expert-driven knowledge base of drug targets and their ligands. Nucl. Acids Res. 42 (Database Issue): D1098–D1106.

Rembold CM (2007). Force suppression and the crossbridge cycle in swine carotid artery. Am J Physiol Cell Physiol 293: C1009–C1009.

Rossin F, D'Eletto M, Falasca L, Sepe S, Cocco S, Fimia GM, *et al*. (2015). Transglutaminase 2 ablation leads to mitophagy impairment associated with a metabolic shift towards aerobic glycolysis. Cell Death Differ 22: 408–418.

Rubin LJ, Magliola L, Feng X, Jones AW, Hale CC (2005). Metabolic activation of AMP kinase in vascular smooth muscle. J Appl Physiol (1985)98: 296–306.

Schaertl S, Prime M, Wityak J, Dominguez C, Munoz-Sanjuan I, Pacifici RE, *et al*. (2010). A profiling platform for the characterization of transglutaminase 2 (TG2) inhibitors. J Biomol Screen 15: 478–487.

Solaro RJ (2000). Myosin light chain phosphatase: a Cinderella of cellular signaling. Circ Res 87: 173–175.

Somlyo AP, Somlyo AV (2003). Ca2+ sensitivity of smooth muscle and nonmuscle myosin II: modulated by G proteins, kinases, and myosin phosphatase. Physiol Rev 83: 1325–1358.

Stack EC, Ferro JL, Kim J, Del Signore SJ, Goodrich S, Matson S, *et al*. (2008). Therapeutic attenuation of mitochondrial dysfunction and oxidative stress in neurotoxin models of Parkinson's disease. Biochim Biophys Acta 1782: 151–162.

van den Akker J, VanBavel E, van Geel R, Matlung HL, Guvenc TB, Janssen GM, *et al*. (2011). The redox state of transglutaminase 2 controls arterial remodeling. PLoS One 6: e23067.

Villalba N, Stankevicius E, Garcia-Sacristan A, Simonsen U, Prieto D (2007). Contribution of both Ca2+ entry and Ca2+ sensitization to the alpha1-adrenergic vasoconstriction of rat penile small arteries. Am J Physiol Heart Circ Physiol 292: H1157–H1169.

Watts SW, Priestley JR, Thompson JM (2009). Serotonylation of vascular proteins important to contraction. PLoS One 4: e5682.

Wilson DP, Susnjar M, Kiss E, Sutherland C, Walsh MP (2005). Thromboxane A2-induced contraction of rat caudal arterial smooth muscle involves activation of Ca2+ entry and Ca2+ sensitization: Rho-associated kinase-mediated phosphorylation of MYPT1 at Thr-855, but not Thr-697. Biochem J 389: 763–774.

Yamada M, Kushibiki M, Osanai T, Tomita H, Okumura K (2008). Vasoconstrictor effect of aldosterone via angiotensin II type 1 (AT1) receptor: possible role of AT1 receptor dimerization. Cardiovasc Res 79: 169–178.

Zhong XZ, Harhun MI, Olesen SP, Ohya S, Moffatt JD, Cole WC, *et al*. (2010). Participation of KCNQ (Kv7) potassium channels in myogenic control of cerebral arterial diameter. J Physiol 588: 3277–3293.

Supporting Information

Additional Supporting Information may be found in the online version of this article at the publisher's web-site:

http://dx.doi.org/10.1111/bph.13393

Figure S1 Relaxations in rat mesenteric arteries with and without endothelium to cystamine in phenylephrine-contracted (A) and U46619-contracted preparations (B), and response in phenylephrine-contracted preparations to (C) acetylcholine, and (D) sodium nitroprusside. Cystamine caused comparable relaxation in vascular segments with and without endothelium. The endothelium was removed by rubbing a small hair against the inner surface of the segment. Vessels with less than 10% relaxation to acetylcholine were considered as without endothelium. **P* <0.05 versus preparations without endothelium. Data are means±SEM of vessel segments from 6 animals.

Figure S2 (A) Effect of a blocker of ATP-sensitive K^+ channels, glibenclamide on levcromakalim relaxations and (B) effect of blockers of large-conductance calcium-activated K^+ channels, tetraethylammonium (TEA) and of K_v7 channels, XE991 on NS11021 in rat mesenteric arteries contracted with phenylephrine. **P* <0.05 versus vehicle incubated preparations. Data are means±SEM of vessel segments from 6 animals.

Figure S3 (A) Representative families of K_v currents in smooth muscle cells isolated from rat mesenteric arteries evoked by voltage steps between -95 and +45 mV. The recordings are made under control conditions, after the application of 10^{-5} M cystamine and following application of 10^{-5} M XE991, as indicated. (B) Averaged I-V relations for K_v currents from the experiments shown in A (n=11).

Figure S4 (A) Time course of increase in phosphorylation of myosin phosphatase targeting subunit 1 (MYPT1- Thr^{855}) following stimulation with 10 μM phenylephrine in rat mesenteric small arteries. Abscissa shows the ratio of phosphorylated-MYPT1/MYPT1 as determined by Western blot in vessels mounted on wire myograph (n=3). (B) Simultaneous measurements of tension, phosphorylation of myosin phosphatase targeting subunit 1 (MYPT1-Thr^{855}), and of phosphorylation of regulatory myosin light chain (MLC2-Ser^{19}) in rat mesenteric arteries contracted with KPSS and then after addition of cystamine (100 μM). Data are means ±SEM of vessel segments from 12 animals.

Figure S5 Average contraction in preparations incubated with phentolamine and vehicle, rotenone, antimycin, the superoxide scavenger, tempol, or the mitochondrial superoxide scavenger, mito-tempo. Contraction were induced with KPSS (100 mM) or in case the incubation affected the contraction level,by KPSS plus U46619 (10^{-7} M). Data are means±SEM of vessel segments from 10 animals. **P* <0.05 versus control.